Journal of Industrial Intelligence
https://www.acadlore.com/journals/JII

Optimization of Magnetically Coupled Resonant Wireless Power Transfer Based on Improved Whale Optimization Algorithm

Yi Du[1*], Jialin Wang[2], Jianguang Lu[3]

[1] School of Electronic Information and Electrical Engineering, Anyang Institute of Technology, 455000 Anyang, China
[2] Kharkiv Institute at Hangzhou Normal University, 311121 Hangzhou, China
[3] Henan Ancai High-Tech Co. LTD, 455000 Anyang, China

[*] Correspondence: Yi Du (20170020@ayit.edu.cn)

Received: 02-12-2023 **Revised:** 03-10-2023 **Accepted:** 03-15-2023

Citation: Y. Du, J. L. Wang, and J. G. Lu, "Optimization of magnetically coupled resonant wireless power transfer based on improved whale optimization algorithm," *J. Ind Intell.*, vol. 1, no. 1, pp. 63–74, 2023. https://doi.org/10.56578/jii010105.

Abstract: This study aimed to address the optimization of magnetically coupled resonant wireless power transfer. An equivalent circuit for the wireless power transfer was established and the factors affecting the transmission efficiency were analyzed. To optimize the system, an improved whale optimization algorithm (WOA) was proposed and applied to optimize the optimal matching values of resonant frequency and load resistance. Performance of the improved WOA was tested using different test functions, and the optimized parameters were applied to the transmission efficiency test of the wireless power transfer system. Experiments demonstrated that the improved WOA effectively optimized the transmission efficiency and achieved good application results in the intelligent transfer system.

Keywords: Magnetically coupled resonant wireless power transfer; Whale optimization algorithm (WOA); Equivalent circuit; Transmission efficiency; Optimization

1 Introduction

Research on wireless energy transfer has become increasingly popular in recent years, as it offers a promising way to improve the performance of energy-constrained low-power systems. Although the use of wireless energy transfer in intelligent pillars has not been extensively studied, it has been applied in other low-power systems, such as wireless communication nodes. Lakhdari et al. [1], Bourouha et al. [2] and Kaur [3] proposed various models for energy harvesting in wireless networks and analyzed their relative strengths and weaknesses. Yao and Ansari et al. [4] developed an adaptive algorithm to optimize the sensing performance of low-power wireless energy transfer systems in sensor networks. Wu et al. [5] studied the use of multiple unmanned aerial vehicles (UAVs) as mobile power sources to wirelessly charge ground-based Internet of Things (IoT) devices, optimizing the UAV trajectories and energy efficiency. Guo et al. [6], Sangare et al. [7], and Dai et al. [8] applied wireless energy transfer in various IoT scenarios and found that it significantly extended the network lifetime of IoT devices. Yuan et al. [9] proposed effective trajectory design for a two-dimensional UAV-assisted wireless energy transfer system with nonlinear ground sensor energy harvesting.

This study focused on the application of wireless energy transfer in intelligent pillars, which presented unique challenges compared with energy supply systems for wireless communication nodes. Therefore, a novel approach based on the WOA was proposed in this study. Originally inspired by the hunting behavior of humpback whales, WOA has shown to be highly competitive compared with other similar optimization algorithms, such as particle swarm optimization (PSO) and gravitational search algorithm (GSA). However, WOA has limitations, such as low global exploration ability and poor optimization accuracy. To overcome these limitations, several modifications of WOA have been proposed, such as the hybrid particle swarm algorithm (HPSO)/whale optimization algorithm (HWOA) by Aljarah et al. [10] and Trivedi et al. [11], the simulated annealing-embedded WOA by Mafarja et al. [12], the sine-cosine-based HWOA by Khalilpourazari and Khalilpourazary [13], the collision-based HWOA by Kaveh and Moghaddam [14], the differential evolution-based HWOA by Bozorgi and Yazdani [15], and the population-based hybrid whale swarm algorithm (WSA) and PSO by Ahmad [16] and Laskar et al. [17]. Abdel-Basset et

al. [18] proposed a new algorithm that combined WOA with a local search strategy to solve permutation flowshop scheduling problems, while Narinder and Hanaa [19] proposed a hybrid algorithm that combined average grey wolf optimization (GWO) and WOA to solve real-life and benchmark problems while addressing the local optima issue.

A modified WOA was proposed in this study, which was specifically tailored to the intelligent pillar energy supply problem. The approach incorporated the strengths of existing WOA modifications and introduced new strategies to improve its performance. Effectiveness of the approach was evaluated through simulations and experiments, and compared with other state-of-the-art algorithms. The results demonstrated the approach was superior in terms of efficiency, accuracy, and robustness.

2 Hardware and Software Design of Intelligent Plunger Resonant Wireless Power Supply

2.1 Hardware Design

Based on the magnetic resonance coupling technology, the magnetically coupled resonant wireless power supply system utilized the coupling relationship between the transmitting and receiving coils to achieve efficient energy transfer under resonant conditions. The supply system was divided into two parts, the transmitting part and the receiving part, as shown in Figure 1.

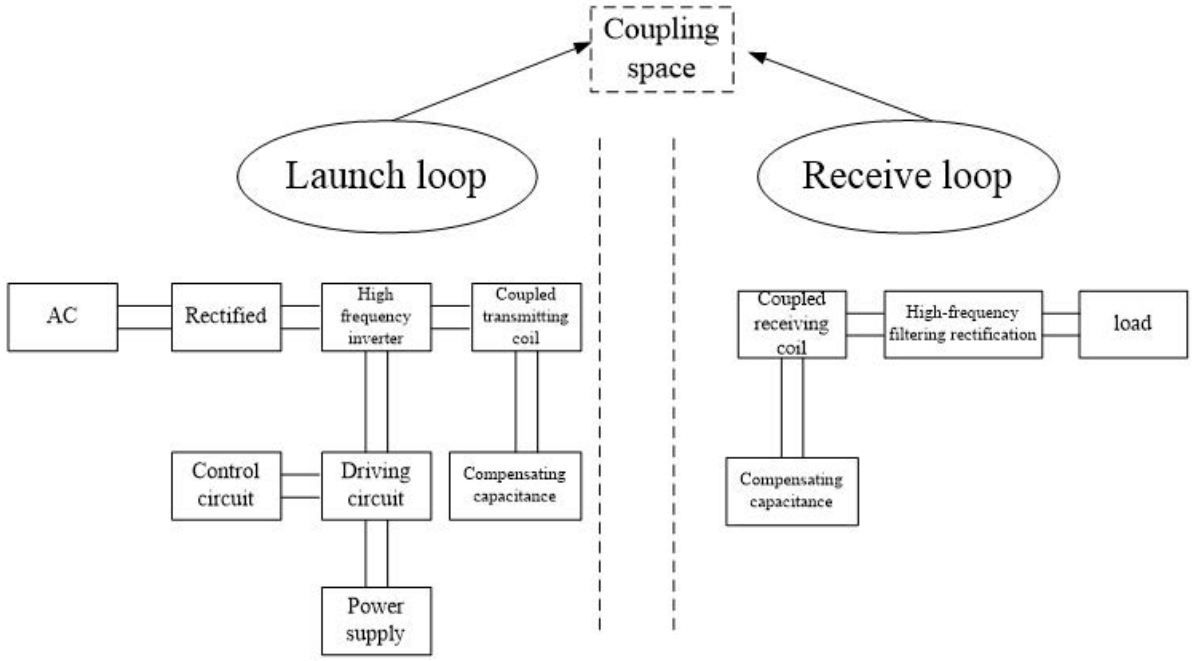

Figure 1. Schematic diagram of the components of magnetically coupled resonant wireless power supply system

The energy transmission circuit included energy supply, filtering and rectification circuit, high-frequency inverter circuit and its driving and control circuit, coupling transmitting coil, and compensation capacitor. The coupling transmitting coil and compensation capacitor mainly constituted the resonant circuit of the transmitting loop. The energy receiving circuit included coupling receiving coil, compensation capacitor, high-frequency filtering and rectification, and load. The coupling receiving coil and compensation capacitor also constituted the resonant circuit of the receiving loop.

2.2 Software Design

2.2.1 Analysis of coil transmission efficiency characteristic

Experimental tests between two coupled coils were conducted in a laboratory environment to analyze the factors affecting their transmission efficiency. After analyzing the impact of different coil radii, the data obtained from the power of the transmitting and receiving loops, and the transmission efficiency under different coil radii was statistically analyzed and calculated. Table 1 shows the results [20, 21].

Figure 2 shows the relationship between coil radius and transmission efficiency tested in the experiment, with coil radius (cm) as the x-coordinate and efficiency (η) as the y-coordinate, based on the data in Table 1.

As shown in Figure 2, the overall system transmission efficiency evidently increases with the increase of the resonant coil radius, though there are some individual deviations in the measured experimental data. The experimental tests were conducted under the condition of equidistant transmission with the same driving voltage. As such, the

Table 1. Experimental test data on radius, number of turns, power, and transmission efficiency

Coil radius (cm)	Coil (number of turns)	Inductance (uH)	Transmission distance (cm)	Transmitting loop power (W)	Receiving loop power (W)	Transmission efficiency (η)
5.0	5	2.03	4	36.5	8.5	23.5%
8.0	5	2.65	4	50.5	15.5	30.5%
10.5	5	3.55	4	70.5	26.2	37.2%
13.5	5	3.85	4	68.6	33.5	48.7%
15.5	5	4.40	4	95.0	38.3	40.2%
18.5	5	5.05	4	71.0	40.2	56.7%
20.0	5	5.92	4	72.2	45.0	62.4%
25.5	5	6.35	4	76.5	52.3	68.5%

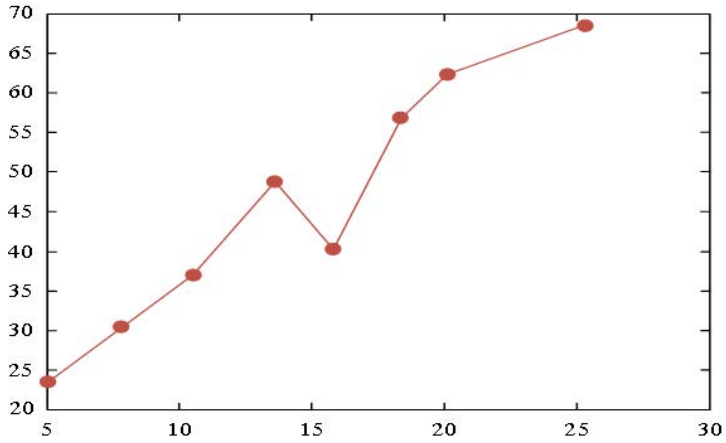

Figure 2. Curve graph of the relationship between coil radius and transmission efficiency

transmission efficiency indirectly measured the coupling degree between the coils, which confirmed the theoretical analysis discussed above, specifically the relationship between coupling degree and radius.

2.2.2 Efficiency characteristics of wireless power transfer frequency

The resonance frequency played an important role in the magnetically coupled resonant energy transfer systems. In wireless energy transfer systems, resonant coupling principles were utilized for wireless electrical energy transmission [22, 23]. The resonant frequency included the self-resonant frequency of coupling transmitting and receiving loops, and the switching frequency of power switches. The resonant state was achieved during circuit operation by adjusting the driving frequency of the inverter circuit for the transmitting and receiving loops. It was observed that the high-frequency driving frequency during normal system operation was usually slightly lower than the resonant frequency of the coupling coils [24, 25]. This study focused on the impact of resonance frequency on the entire system, particularly load absorption power and transmission efficiency. When the system circuit operated in a resonant state, the resonant frequency obtained was $\omega = \frac{1}{\sqrt{L_1 C_1}} = \frac{1}{\sqrt{L_2 C_2}}$, and the absorbed power of the load in the resonant state was:

$$P_{\text{out}} = \frac{U_{\text{in}}^2 (\omega M)^2 R_0}{\left[R_1 (R_0 + R_2) + (\omega M)^2\right]^2} \tag{1}$$

After analyzing the parameter relationship between the transmission efficiency n and f frequency in the resonant state of the wireless power transfer system, it was concluded that the system transmission efficiency was regarded as the ratio of the load absorption power to the transmitting loop power. The calculation expression for the transmission efficiency was obtained as:

$$\eta = \frac{(\omega M)^2 R_0}{(R_0 + R_2)\left[R_1 (R_0 + R_2) + (\omega M)^2\right]} \times 100\% \tag{2}$$

The formula for calculating the transmission efficiency was optimized to obtain the maximum value at $\omega = \frac{\sqrt{R_1 (R_0 + R_2)}}{M}$, which indicated that the system achieved the highest transmission efficiency at this frequency. The

relationship among the transmission efficiency, frequency, and load at this point was studied. Experimental data was collected and analyzed. Figure 3 shows the relationship among transmission efficiency η, frequency $\frac{f}{f_0}$, and load R_0, with frequency $\frac{f}{f_0}$ as the x-coordinate and efficiency η as the y-coordinate.

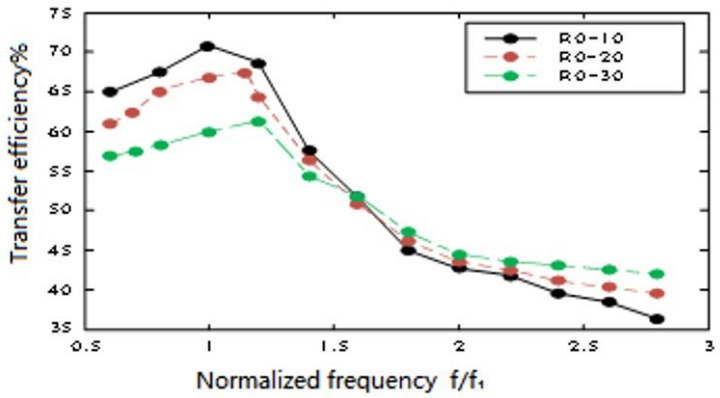

Figure 3. Relationship among transmission efficiency η, frequency $\frac{f}{f_0}$, and load R_0

According to the results in Figure 3, it is evident that the system has achieved the maximum transmission efficiency η when operating at the resonant frequency f_0. As the frequency deviated from the resonant frequency, the transmission efficiency gradually decreased. The relationship between the transmission efficiency η and the load was relatively complex. Specifically, the system had higher transmission efficiency and smaller loads when the resonant frequency was $\frac{f}{f_0} < 1$, and higher transmission efficiency and larger loads when the resonant frequency was $\frac{f}{f_0} > 1$.

Furthermore, the same experimental method was used to study the relationship among transmission efficiency η, load R_0, coil internal resistance R_1 and R_2. Figure 4 presents the obtained relationship, with load $R_0(\Omega)$ as the x-coordinate and efficiency η as the y-coordinate.

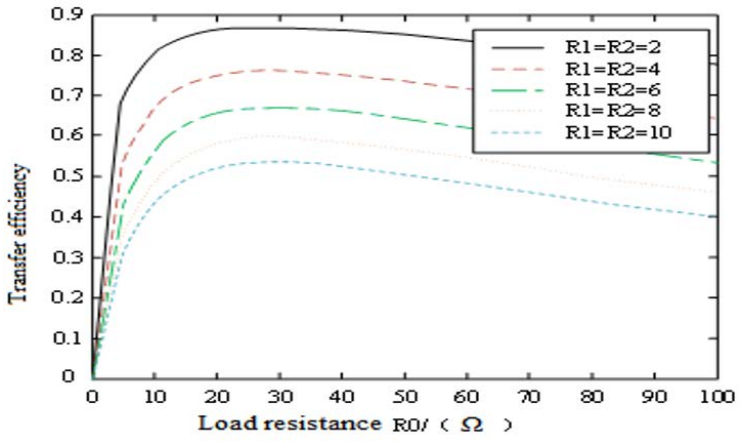

Figure 4. Relationship among transmission efficiency η, load R_0, coil internal resistance R_1 and R_2

Figure 4 shows the relationship among transmission efficiencyη, loadR_0, coil internal resistance R_1 and R_2. According to the figure, it can be concluded that larger loads do not necessarily lead to better performance of circuit transmission efficiency, as there is an optimal matching value. Additionally, the coil internal resistance has an inverse relationship with the energy transfer efficiency, meaning that the efficiency decreases with the increase of resistance. Therefore, it was recommended to use coils with larger wire diameter in experiments, and the load design should take into account the actual circuit parameters, such as resonant frequency, transmission distance, transmitting power, and coil parameters.

2.2.3 Mathematical model

The objective function was:

$$\max(f) = \frac{R_L |I_2|^2}{\text{real}\,(U_s \cdot I_1^*)} \tag{3}$$

The constraint conditions were:

$$0 < d < 200 \tag{4}$$

$$0 < R_L < 150 \tag{5}$$

$$0 \leq \omega \leq 100 \tag{6}$$

In the transmission efficiency objective function (3), $R_L \left|I_2\right|^2$ and $\operatorname{real}\left(U_s \cdot I_1^*\right)$ represent the active power of both the system load and the transmitting part of the system, respectively.

In the constraint condition (4), d represents the transmission distance, which ranges from 0 to 200mm. In the constraint condition (5), R_L represents the load resistance, which ranges from 0 to 150Ω. In the constraint condition (6), ω represents the resonant frequency of the parameter, which ranges from 0 to 100. The upper and lower limits of the parameters were determined based on the specific situation of the cylindrical wireless power supply system.

2.2.4 Improvement of the WOA design

Inspired by the hunting behavior of whales, the WOA is a novel intelligent optimization algorithm and has many advantages, such as fewer parameters, a fast convergence speed, and high precision. In the algorithm, the individual position of each whale represents a target solution to the optimization problem. Whales surround and capture their prey by moving towards their locations. In optimization problems, the prey represents the current optimal solution, and each whale in the population moves towards it during the iterative process.

Although WOA is a simple and easy-to-implement meta-heuristic algorithm with superior performance in accuracy and convergence speed, compared with particle swarm algorithm and GSA, it has limitations in solving complex problems or high-dimensional space searches. The abstraction of the whale hunting behavior into a mathematical model is suitable for analyzing simple optimization problems, but it can lead to insufficient global search capability, low convergence accuracy, and a tendency to get stuck in local optima.

The following steps were taken to improve the WOA's ability to optimize the parameter values of a magnetically coupled resonant wireless power transfer system:

(1) A non-linear convergence factor was introduced to improve the convergence speed of the optimal solution in the global search domain. Coefficient vector determined the global search capability of WOA. If the convergence factor decreased linearly during the WOA operation, it easily got stuck in a local search in the later iteration stage. By introducing the segmented convergence factor, the global search capability of WOA was improved without affecting its convergence speed in the later stage.

(2) Based on the study of population diversity in biology, the population clustering degree metric 1/k was introduced to avoid premature convergence of individuals and promote diversity in the search process. This metric was used to guide the mutation operation and promote the population diversity. The steps for improving the WOA were as follows:

Step 1

Let *N* be the whale population size, *T* be the maximum iteration number, *LB* and *SB* be the upper and lower bounds of optimization variables, dim be the search space dimension, δ and d be the search step size and spacing. After initializing them, the whale population was randomly generated and defined as follows:

$\lambda_i^t = x_i^t \quad \mathrm{i} = 1, 2, \ldots\ldots \mathrm{N} \quad x_i^t \in [LB, SB]$

where, *t* is the iteration number, λ_I^t is the *i-th* whale solution in the whale population during the *t-th* iteration, and x_i^t is the transmitting coil efficiency for the *i-th* whale solution in the whale population during the *t-th* iteration.

Step 2

According to the output power model described in Step 1, the fitness value of each whale in the search space $f\left(x_i^t\right)$, i.e., for i = 1, 2, ..., N, was calculated, and the whale with the minimum fitness value was recorded as x^*.

Step 3

Let a be the convergence factor, *A* and *C* be the position update parameters, *L (L∈[1,1])* and *p (p∈[0,1])* be the random variables. When iteration started and the parameters and variables were updated, the specific expressions were as follows:

$$\begin{cases} x(t+1) = x_{\text{best}}(t) - A \times D \\ D = \left|C \times x_{\text{best}}(t) - x(t)\right| \\ A = 2 \times a \times r_1 - a \\ C = 2 \times r_2 \\ a = 2 - 2 \times t / t_{\max} \end{cases} \tag{7}$$

where, t and $t_{\max}$ are the current and the maximum iteration numbers, $x(t)$ is the whale position, $x_{\text{best}}(t)$ is the global best position, A and C are coefficient matrices, r_1 and r_2 are the uniformly distributed random numbers in the range [0,1], α is the convergence factor linearly decreasing from 2 to 0, which can control the probability of whales randomly searching or enclosing prey, and p is an uniformly distributed random number in the range [0,1].

Step 4

During the process of approaching prey, whales moved in a spiral manner to search the possible optimal solution in the search path. The position update method is shown in equation (4). When $\mathrm{p} > 0.5$, the whale moved according to its current method.

$$x(t+1) = x_{\text{best}}(t) - D \times e^{bl} \times \cos 2\pi l \tag{8}$$

where, the constant *b* is set to 1, which can change the spiral shape, and *l* is an uniformly distributed random number in the range [-1,1]. Whales moved towards a random individual direction for global search. The position update method is shown in equation (10), where the whale moves according to its current method when $\mathrm{p} < 0.5$ and $\mathrm{r} < 0.5$.

$$x(t+1) = x_{\text{rand}}(t) - A \times |C \times x_{\text{rand}}(t) - x(t)| \tag{9}$$

where, $x_{\text{rand}}(t)$ represents a random whale position.

Step 5

The introduced convergence factor was:

$$a(\varepsilon) = \begin{cases} 2 - \left(\frac{\varepsilon}{M}\right)^2, \varepsilon \le \frac{M}{2} \\ 1 - \frac{2\left(\varepsilon - \frac{\varepsilon}{M}\right)}{M} + \left(\frac{\varepsilon - \frac{M}{2}}{M}\right), \varepsilon > \frac{M}{2} \end{cases} \tag{10}$$

where, *M* is the maximum iteration number. The algorithm was optimized based on the analysis of its iteration process.

Step 6

According to the operating principle of the algorithm, the degree of population clustering was expressed as:

$$\frac{1}{k} = \frac{V - m}{m^2} \tag{11}$$

where, *V* represents the fitness variance of the population, and *m* represents the fitness mean of the population.

When $\frac{1}{k} >> 0$, the population was in a clustered state, while $\frac{1}{k} \to 0$ represented a random state of the population that required global search. To avoid clustering in the early iteration stage and promote population diversity, a mutation operation was applied to the population in early iteration stage (i.e $\le M/2$), with a mutation threshold set as $\frac{1}{k} = 0.125$. The equation was as follows:

$$X(\varepsilon + 1) = X(\varepsilon) \cdot (1 + 0.5\zeta) \tag{12}$$

where, ζ is a random variable following negative binomial distribution.

Step 7

It was checked whether the maximum iteration number had been reached or not. If so, the optimal whale position was output, which represented the optimal solution. Figure 5 shows the process of improving the WOA.

2.3 Simulation Verification and Result Analysis

All experiments in this study were conducted in the same environment, i.e. an Intel Core (TM) i7-6700 central processing unit running at a frequency of 3.40GHz, 8.00GB of RAM, and the Windows 10 operating system. Matlab was used as the development language.

2.4 Parameter Matching Optimization Method

The parameters of a magnetically coupled resonant wireless power transfer system, which affected the transmission efficiency, needed to be optimized using the improved WOA, such as the resonance frequency ω, load resistance R_L, and transmission distance *d* in Eq. (14):

$$x_i^3 = [d, \omega, R_L] \tag{13}$$

According to the transmission efficiency analysis of magnetically coupled systems, the resonance frequency, load resistance, and magnetic coupling transmission distance had a significant impact on the transmission efficiency. The frequency transmission characteristics of the system were analyzed in combination with a single load and an concatenation-concatenation resonance compensation circuit structure.

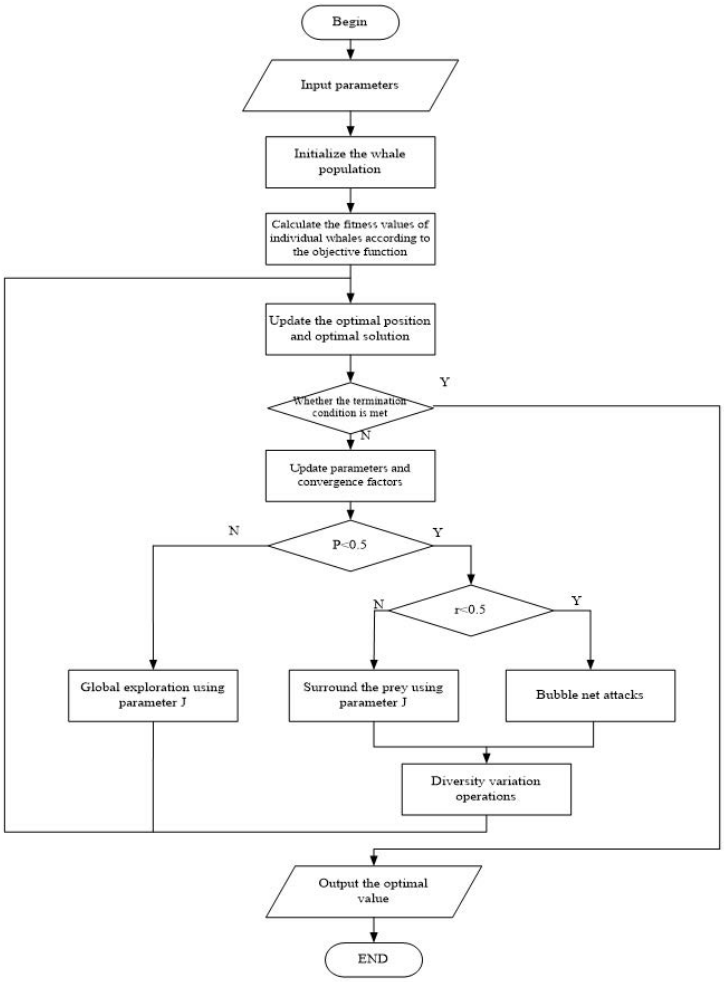

Figure 5. Flowchart of the improved WOA

In the MATLAB simulation software, the system had 220V/50Hz working voltage, 10Ω load resistance, $R_1 = R_2 = 0.02\Omega$ coil resistance, and 0.1 coupling coefficient between the transmitter and receiver coils. After changing the working frequency in the range from 0 to 100kHz, the relationship among the output power, transmission efficiency, and frequency of the magnetically coupled resonant wireless power transfer system was obtained, as shown in Figure 6 and Figure 7, with resonance frequency (kHZ) as the x-coordinate, and power transfer system (kW) as the y-coordinate in Figure 6 and efficiency η .as the y-coordinate in Figure 7, respectively.

Based on the obtained relationship curves between the output power and frequency, and that between the transmission efficiency and frequency of the magnetically coupled resonant wireless power transfer system, the maximum output power point and the maximum transmission efficiency point were identified. It was found that the frequencies corresponding to these two points were roughly the same, and were located near the resonance frequency of the system.

At the resonance frequency, the relationship curve between the transmission efficiency and load resistance was obtained by adjusting the load resistance, as shown in Figure 8, with load resistance (Ω) as the x-coordinate and efficiency η as the y-coordinate.

According to the results in Figure 8, it can be observed that the transmission efficiency of the magnetically coupled resonant wireless power transfer system sharply increases as the load resistance increases from 0 when the system operates at the resonance frequency. However, when the load resistance reaches a certain value, the transmission efficiency also reaches its maximum value. As the load resistance continues to increase beyond this point, the transmission efficiency starts to decrease.

Regarding the relationship between the transmission efficiency and distance of the system, this study mainly paid attention to the axial distance between the transmitter and receiver coils. By setting the same parameters for both coils, the relationship curve between their axial distance (i.e., the transmission distance) and the transmission efficiency was obtained, as shown in Figure 9, with transmission distance as the x-coordinate and efficiency η as the y-coordinate.

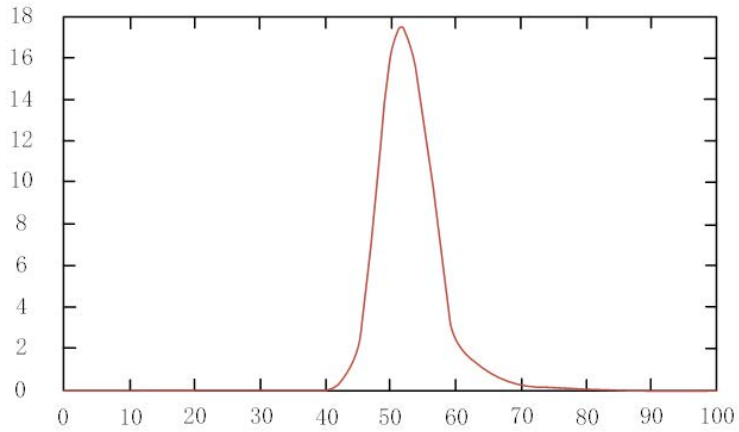

Figure 6. Relationship curve between output power and resonance frequency of magnetically coupled resonant wireless power transfer system

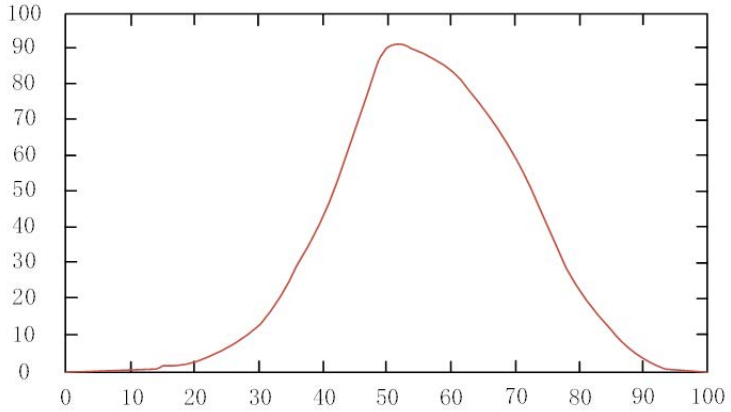

Figure 7. Relationship curve between transmission efficiency and resonance rrequency of magnetically coupled resonant wireless power transfer system

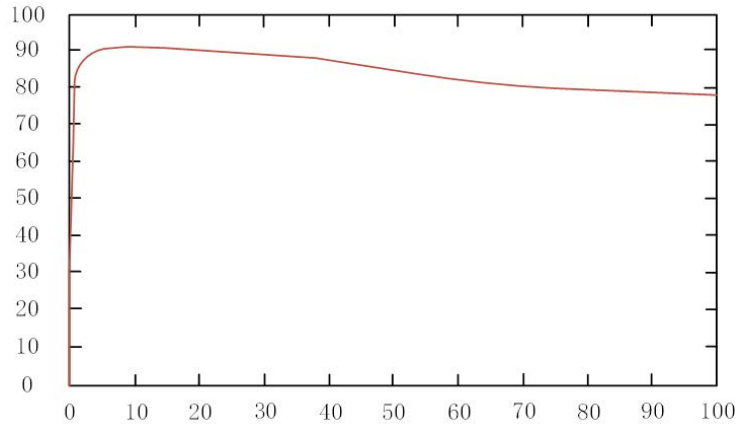

Figure 8. Relationship curve between transmission efficiency and load resistance of magnetically coupled resonant wireless power transfer systemm

Figure 9 shows the complex relationship between the transmission efficiency and distance of the system. When the distance between the coils increased initially, the transmission efficiency also increased. However, when the distance continued to increase, the transmission efficiency started to decrease at a certain point.

According to the coupling coefficient between the coils $k = M\sqrt{L_1 L_2}$, the distance between the coils affected their coupling rate. When the distance between the coils was shorter, the coupling rate was higher, which led to

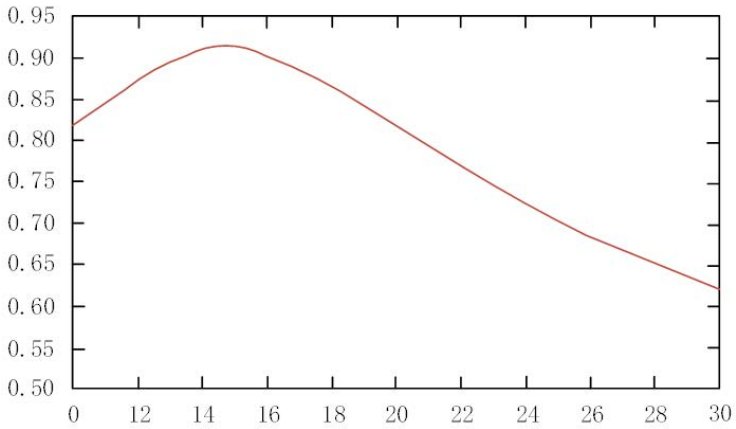

Figure 9. Relationship curve between transmission efficiency and distance of magnetically coupled resonant wireless power transfer system

better transmission efficiency. However, the system entered an overcoupling state after reaching a critical coupling point. Beyond this point, with the decrease of the distance between the coils, the coupling rate started to decrease as well. Therefore, the transmitter and receiver coils should be ensured to operate at the critical coupling state to improve the transmission efficiency.

2.5 Simulation and Result Analysis

In MATLAB simulation, it is observed from Figure 10 that the parameter of transmission distance (d) has a high transmission efficiency within the range of [10cm, 20cm]. Outside this range, the transmission efficiency is not satisfactory. Figures 7 and 8 show that the working frequency has a higher output power and transmission efficiency within the range of [40 kHz, 60 kHz]. According to Figure 9, the load resistance has a higher transmission efficiency within the range of $[2\Omega, 20\Omega]$. Therefore, the constraints were modified as follows:

$$10 < d < 24 \tag{14}$$

$$2 < R_L < 20 \tag{15}$$

$$40 \leq \omega \leq 60 \tag{16}$$

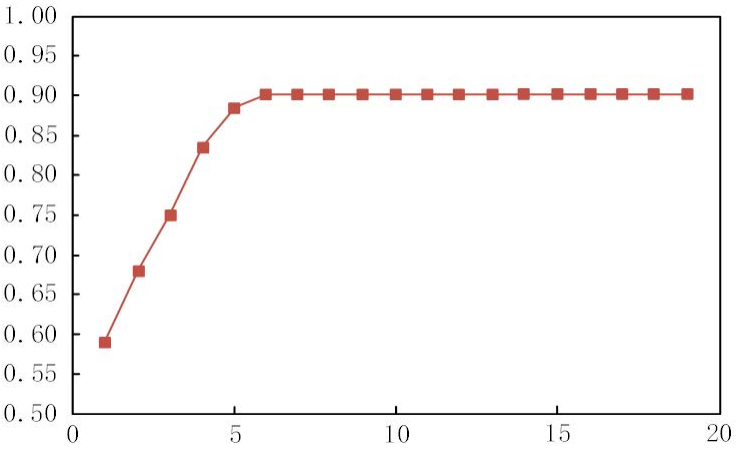

Figure 10. Transmission efficiency curve of the system

Following the steps of the improved WOA and the flowchart in Figure 6, a whale population of 30 was initialized with the maximum iteration of 50. The upper bounds for the optimized variables were set to be 20, 20, and 60, respectively, while the lower bounds were set to be 10, 0, and 40. The search space dimension was 3. The search step size was initialized to be 1, and the resulting table data was as follows:

Table 2. Table of improved WOA data

d / cm	R_L / Ω	ω / kHZ	Output power / kW	Efficiency / %
10	2	40	4	20
10	2	41	4.2	21
10	3	41	4.21	21
11	3	41	4.3	21.5
11	3	42	4.5	22.5
11	4	42	5	25
12	4	42	5.5	27.5
12	4	43	6.1	30.5
12	5	43	6.7	33.5
13	5	43	7	35
13	5	44	7.7	38.5
13	6	44	8	40
14	6	44	9	45
14	6	45	9.5	47.5
14	7	45	10	50
15	7	45	11	55
15	7	46	11.5	55.5
15	8	46	12	56
16	8	46	12.7	56.7
16	8	47	13	65
16	9	47	13.6	67
17	9	47	14	70
17	9	48	15	75
17	10	48	15.9	79.5
18	10	48	16.8	84.5
18	10	49	17.5	87.5
18	11	49	18	90
19	11	49	18	90
19	11	50	18.2	90.1
19	14	50	17.7	88.2
19	14	50	17 .	85
20	14	54	16	80
20	16	54	15.5	78.5
20	16	54	14	70
22	16	57	10	50
22	20	57	8	40
22	20	57	6	30
24	20	60	3	25

Table 2 shows that the optimized parameter values are 19cm, 11Ω, and 50 kHz. Then these values were used to simulate the system's transmission efficiency. Figure 10 shows the results, with number of iterations as the x-coordinate and efficiency η as the y-coordinate.

As shown in Figure 10, the improved WOA converges within 20 iterations. With the increase of the iteration number, the transmission efficiency improved. When the algorithm iterated six times, the transmission efficiency was guaranteed to be above 90%, which demonstrated the effectiveness of the improved WOA in optimizing the parameters of the magnetic resonant wireless power transfer system.

3 Conclusion

This study focused on characteristics of the magnetic resonant wireless power transfer system, by taking into consideration power supply requirements of the intelligent plunger automatic control system for natural gas extraction. A brief analysis of the system was presented, along with a detailed explanation of the theoretical and main transmission structures involved. After analyzing the influencing factors of the magnetic resonant wireless power transfer system, an equivalent circuit for the magnetic resonant wireless power transfer was established. Coupling characteristics of the commonly used parallel coil structure were analyzed, including coil mutual inductance, transmission efficiency, and capacitance coupling, and the relationship among these characteristics was discussed. The SS resonance

compensation method was selected to analyze the key parameters, which affected the transmission efficiency of the wireless power transfer system. Frequency efficiency characteristics of the wireless power transfer transmission and the transmission efficiency improvement measures were summarized. An improved WOA was utilized to optimize the resonant frequency and load resistance matching values, and the performance of the improved WOA was tested using different test functions. Then the obtained optimized parameters were used to test the transmission efficiency of the wireless power transfer system, which proved the improved WOA was effective in optimizing system parameters. Although some results have been achieved in the study on the intelligent plunger wireless power supply technology, improvements are still necessary in certain aspects. Future research will focus on more design studies on wireless power supply systems by using magnetic resonant wireless power transfer, analyzing and designing the main circuit modules, along with studying the losses of the switching devices in the system to ensure stable operation at the resonant frequency point, in combination with the frequency tracking control algorithm for the intelligent plunger during the entire charging and leaving process. Additionally, more intelligent algorithms will be utilized to do research on system parameter optimization based on the characteristics of the WOA, providing optimization results based on practical testing.

Data Availability

The data used to support the findings of this study are available from the corresponding author upon request.

Conflicts of Interest

The authors declare that they have no conflicts of interest.

References

[1] A. Lakhdari, N.-E. M. Maaza, and M. Dekmous, "Design and optimization of inductively coupled spiral square coils for bio-implantable micro-system device," *Int. J. Electr. Comput. Eng.*, vol. 9, no. 4, pp. 2637–2647, 2019. https://doi.org/10.11591/ijece.v9i4.pp3189-3196

[2] M. A. Bourouha, M. Bataineh, and M. Guizani, "Advances in optical switching and networking: past, present, and future," *In Proceedings IEEE SoutheastCon 2002 (Cat. No. 02CH37283)*, pp. 405–413, 2002. https://doi.org/10.1109/SECON.2002.995629

[3] P. Kaur, B. S. Sohi, and P. Singh, "Recent advances in mac protocols for the energy harvesting based wsn: A comprehensive review," *Wireless Personal Communications*, vol. 104, pp. 423–440, 2019. https://doi.org/10.1007/s11277-018-6028-3

[4] J. Yao and N. Ansari, "Caching in energy harvesting aided internet of things: A game-theoretic approach," *IEEE Internet Things*, vol. 6, no. 2, pp. 3194–3201, 2018. https://doi.org/10.1109/JIOT.2018.2858763

[5] P. Wu, F. Xiao, H. Huang, C. Sha, and S. Yu, "Adaptive and extensible energy supply mechanism for uavs-aided wireless-powered internet of things," *IEEE Internet Things*, vol. 7, no. 9, pp. 9201–9213, 2020. https://doi.org/10.1109/JIOT.2020.3005133

[6] S. Guo, C. Wang, and Y. Yang, "Joint mobile data gathering and energy provisioning in wireless rechargeable sensor networks," *IEEE Trans. Mobile Comput.*, vol. 13, no. 12, pp. 2836–2852, 2014. https://doi.org/10.1109/TMC.2014.2307332

[7] F. Sangare, Y. Xiao, D. Niyato, and Z. Han, "Mobile charging in wireless-powered sensor networks: Optimal scheduling and experimental implementation," *IEEE Trans. Veh. Technol.*, vol. 66, no. 8, pp. 7400–7410, 2017. https://doi.org/10.1109/TVT.2017.2668990

[8] H. Dai, X. Wu, G. Chen, L. Xu, and S. Lin, "Minimizing the number of mobile chargers for large-scale wireless rechargeable sensor networks," *Comput. Commun.*, vol. 46, pp. 54–65, 2014. https://doi.org/10.1016/j.comcom.2014.03.001

[9] X. Yuan, T. Yang, Y. Hu, J. Xu, and A. Schmeink, "Trajectory design for uav-enabled multiuser wireless power transfer with nonlinear energy harvesting," *IEEE Trans. Wireless Commun.*, vol. 20, no. 2, pp. 1105–1121, 2020. https://doi.org/10.1109/TWC.2020.3030773

[10] I. Aljarah, H. Faris, and S. Mirjalili, "Optimizing connection weights in neural networks using the whale optimization algorithm," *Soft Comput.*, vol. 22, pp. 1–15, 2018. https://doi.org/10.1007/s00500-016-2442-1

[11] I. N. Trivedi, P. Jangir, A. Kumar, N. Jangir, and R. Totlani, "A novel hybrid pso–woa algorithm for global numerical functions optimization," pp. 53–60, 2018. https://doi.org/10.1007/978-981-10-3773-3_6

[12] M. Mafarja, I. Jaber, S. Ahmed, and T. Thaher, "Whale optimisation algorithm for high-dimensional small-instance feature selection," *International Journal of Parallel, Emergent and Distributed Systems*, vol. 36, no. 2, pp. 80–96, 2021.

[13] S. Khalilpourazari and S. Khalilpourazary, "Scwoa: an efficient hybrid algorithm for parameter optimization

of multi-pass milling process," *J. Ind. Prod. Eng.*, vol. 35, no. 3, pp. 135–147, 2018. https://doi.org/10.1080/21681015.2017.1422040

[14] A. Kaveh and M. Rastegar Moghaddam, "A hybrid woa-cbo algorithm for construction site layout planning problem," *Sci Iran.*, vol. 25, no. 3, pp. 1094–1104, 2018. https://doi.org/10.24200/SCI.2017.4212

[15] S. Mostafa Bozorgi and S. Yazdani, "Iwoa: An improved whale optimization algorithm for optimization problems," *Journal of Computational Design and Engineering*, vol. 6, no. 3, pp. 243–259, 2019. https://doi.org/10.1016/j.jcde.2019.02.002

[16] W. Chen, H. Hong, M. Panahi, H. Shahabi, Y. Wang, A. Shirzadi, S. Pirasteh, A. A. Alesheikh, K. Khosravi, S. Panahi *et al.*, "Spatial prediction of landslide susceptibility using gis-based data mining techniques of anfis with whale optimization algorithm (woa) and grey wolf optimizer (gwo)," *Appl Sc.*, vol. 9, no. 18, p. 3755, 2019. https://doi.org/10.3390/app9183755

[17] N. M. Laskar, K. Guha, I. Chatterjee, S. Chanda, K. L. Baishnab, and P. K. Paul, "Hwpso: A new hybrid whale-particle swarm optimization algorithm and its application in electronic design optimization problems," *Appl. Intell.*, vol. 49, pp. 265–291, 2019. https://doi.org/10.1007/s10489-018-1247-6

[18] M. Abdel-Basset, G. Manogaran, D. El-Shahat, and S. Mirjalili, "Retraction notice to "a hybrid whale optimization algorithm based on local search strategy for the permutation flow shop scheduling problem"," *Future Gener. Comput. Syst.*, pp. 129–145, 2022. https://doi.org/10.1016/j.future.2022.05.029

[19] N. Singh and H. Hachimi, "A new hybrid whale optimizer algorithm with mean strategy of grey wolf optimizer for global optimization," *Math. Comput. Appl.*, vol. 23, no. 1, p. 14, 2018. https://doi.org/10.3390/mca23010014

[20] Y. Liu, M. Chen, and M. Jiang, "Laser energy supply electronic current transformer photoelectric transmission system based on energy transfer fiber," *Electron. Des. Eng.*, vol. 16, no. 3, p. 30, 2022.

[21] L. Diao, Y. Zhang, and Z. Jin, "Adaptive optimization method and system for energy management of hybrid energy supply system," 2022, cN115330052A.

[22] L. Diao, Y. Zhang, and Z. Jin, "Uav-assisted wireless power iot energy optimization based on stackelberg game," *J. Commun.*, vol. 43, no. 12, p. 11, 2022.

[23] B. Liu, "Application of wireless private network in energy internet smart park," *Electromech. Technol. Hydropower Plants*, vol. 44, no. 1, pp. 11–15, 2021.

[24] M. Zhao, Y. Liu, and Z. Guoqing, "Multi objective optimization of distributed energy supply network based on energy interconnection," *Power Technol. Environ. Protect.*, vol. 37, no. 6, pp. 40–50, 2021.

[25] X. Xue, Y. Zheng, and C. Lu, "Optimal allocation of distributed energy supply system under uncertainty based improved gray wolf algorithm," *Distrib. Gener. Altern. Energy J.*, vol. 37, pp. 381–400, 2022. https://doi.org/10.13052/dgaej2156-3306.37215